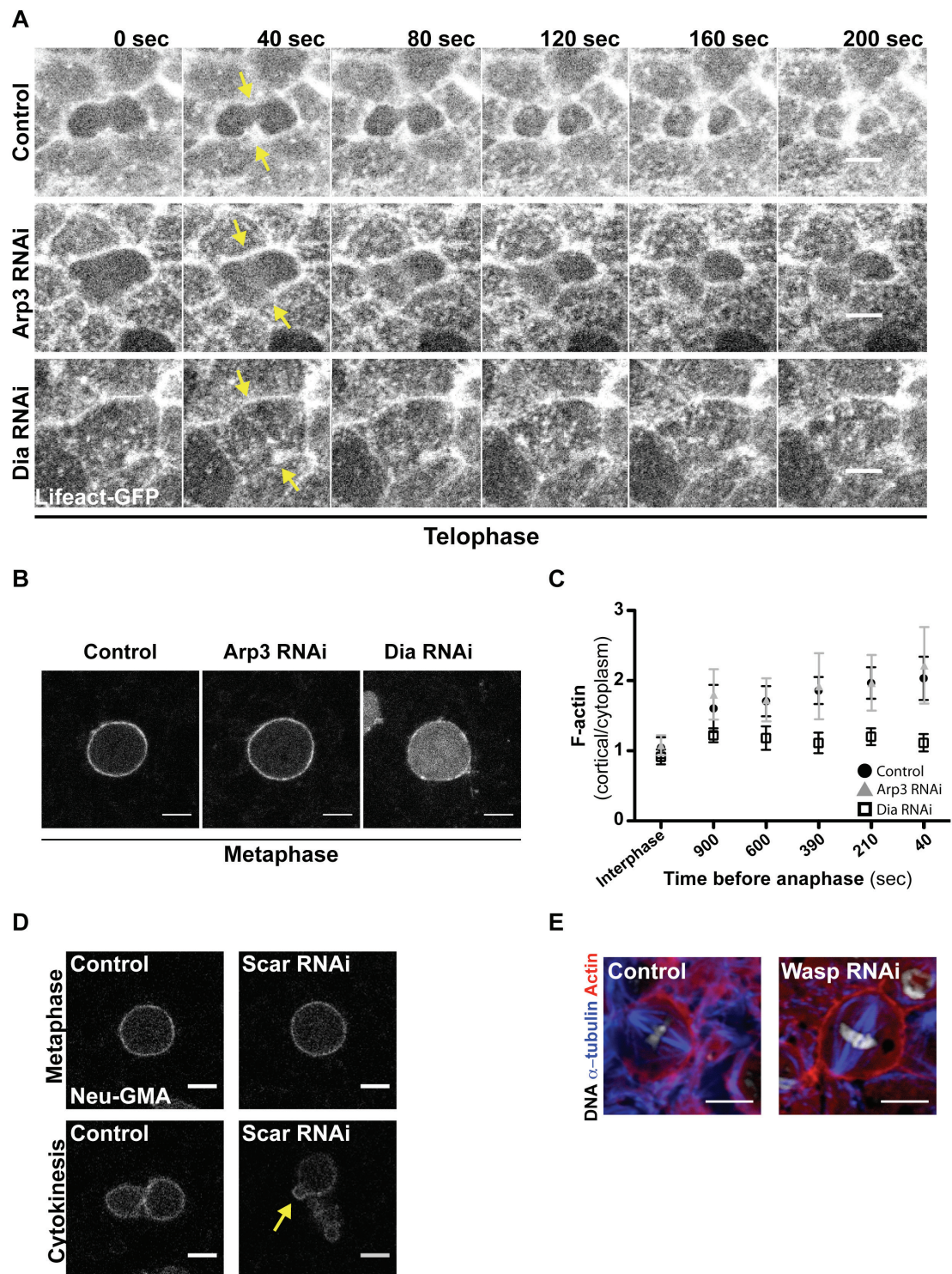


Developmental Cell

Supplemental Information

**Ect2/Pbl Acts via Rho and Polarity Proteins  
to Direct the Assembly of an Isotropic  
Actomyosin Cortex upon Mitotic Entry**

André Rosa, Evi Vlassaks, Franck Pichaud, and Buzz Baum



**Figure S1. The Arp2/3 complex is not required for the assembly of a mitotic actin cortex; Related to Fig.2. (A)** Time-lapse shows the apical portion of a cell expressing UAS-Lifeact::GFP together with *arp3* or *dia* dsRNA imaged in the plane of the epithelium. Time T=0 sec indicates the

onset of cytokinesis. Yellow arrow points to furrowing in control and Arp3 RNAi cells and to the equivalent region of Dia RNAi cells. **(B)** Metaphase cells viewed in the plane of the epithelium expressing UAS-GMA (control) to label F-actin together with Arp3 or Dia RNAi. **(C)** Graph indicates the cortical/cytoplasm ratio of F-actin intensity in the spindle plane as control, Arp3 and Dia RNAi cells enter mitosis. (Mean $\pm$ SD, N $\geq$ 25 cells from at least 3 different pupae). **(D)** The cortex of control (Neu:GMA) and SCAR RNAi cells in mitosis and following mitotic exit imaged at the level of the spindle in xy. **(E)** Control and Wasp RNAi cells imaged in the plane of the epithelium stained for filamentous actin (red), DNA (white) and  $\alpha$ -tubulin (blue). Scale bar: 5  $\mu$ m.



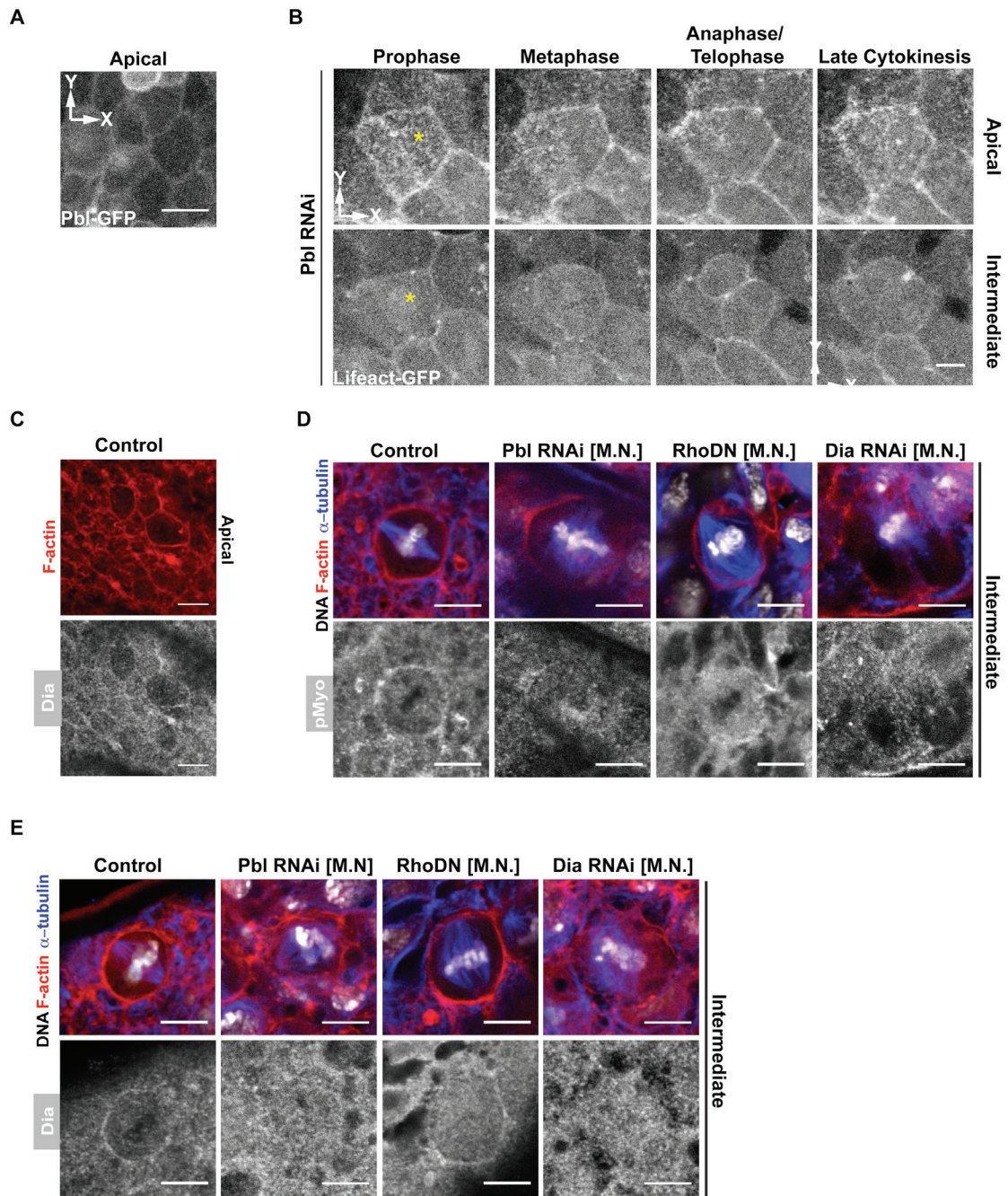


**Figure S2. Pbl/Ect2 is required for the correct cortical localization of Dia and Myosin-II; Related to Fig.3. (A)** An apical section showing interphase epithelial cells expressing low levels of UAS-Pbl::GFP imaged in the plane of the epithelium. **(B)** Characteristic hypomorphic Pbl RNAi phenotype in a cell labelled with UAS-Lifeact::GFP (as seen in Figure 3) imaged at apical and intermediate sections in the plane of the epithelium. Yellow asterisk indicates a dividing cell. **(C)** Apical section of tissue to show the localization of F-actin (red) and Diaphanous (white) during interphase. **(D)** F-actin (red), DNA



(white),  $\alpha$ -tubulin (blue) and phospho-Myosin-II (white) in control, Pbl RNAi, Dia RNAi and Rho1.N19 expressing cells at metaphase. **(E)** As for D, but with Diaphanous shown in white. M.N. = Multinucleated. Scale bar: 5  $\mu$ m.

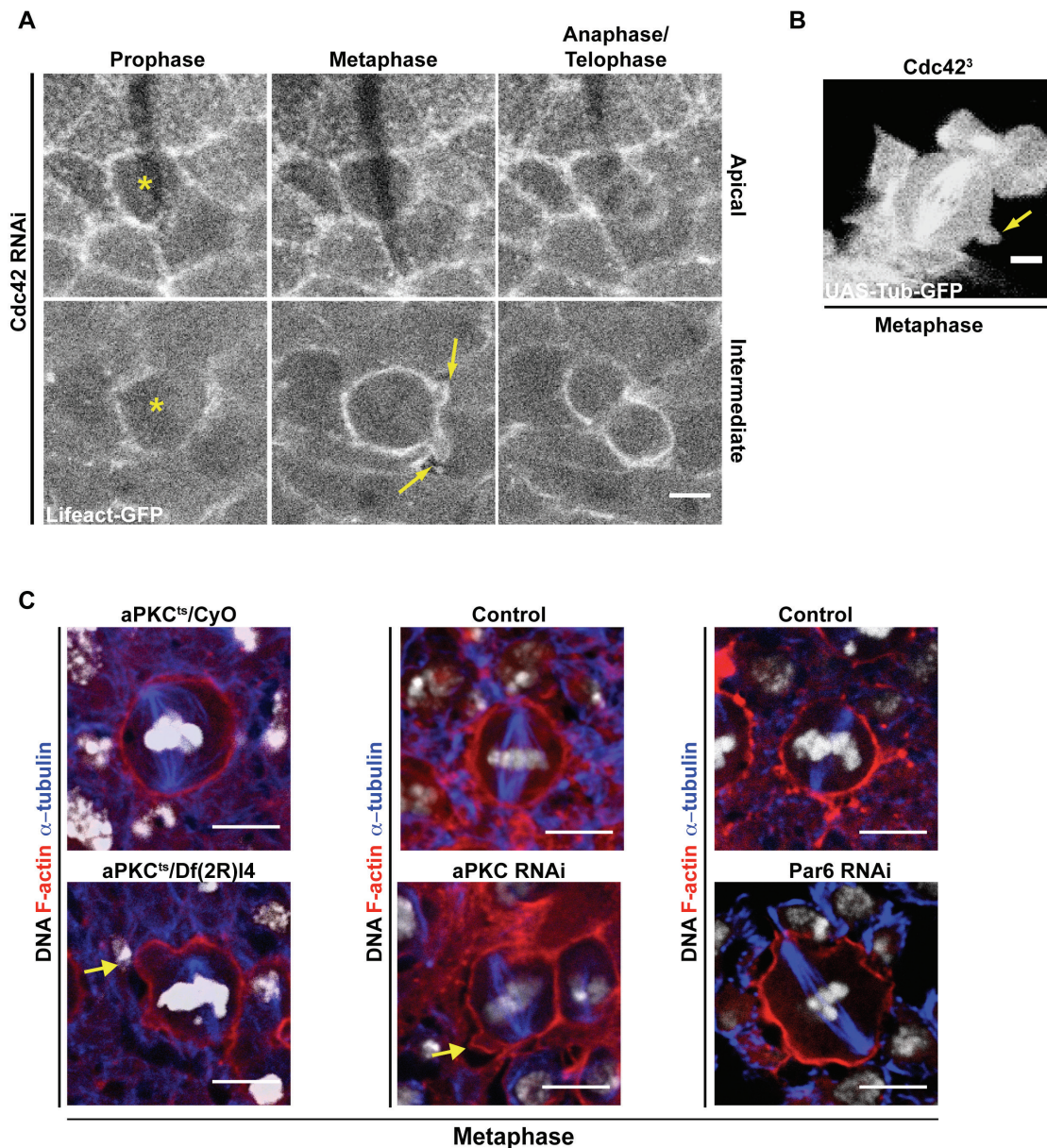


**Figure S3. Cdc42, aPKC and Par6 control actin cortex stability; Related to Fig.4.** (A) Apical and spindle-level (intermediate) views in the plane of the epithelium for Cdc42 RNAi cells expressing UAS-Lifeact::GFP at different stages of mitosis (as seen in Figure 4). Yellow asterisk indicates dividing cell. Yellow arrows indicate blebbing. (B) Mosaic clone of marked *cdc42*<sup>3</sup> cells expressing UAS-Tub::GFP viewed in xy. Yellow arrow indicates metaphase bleb. (C) Control, aPKC RNAi, Par6 RNAi and homozygous *aPKC*<sup>ts</sup> mutant cells in metaphase labelled to show F-actin (red), DNA (white) and  $\alpha$ -tubulin (blue). Yellow arrows indicate cell shape deformations. Scale bar: 5  $\mu$ m.



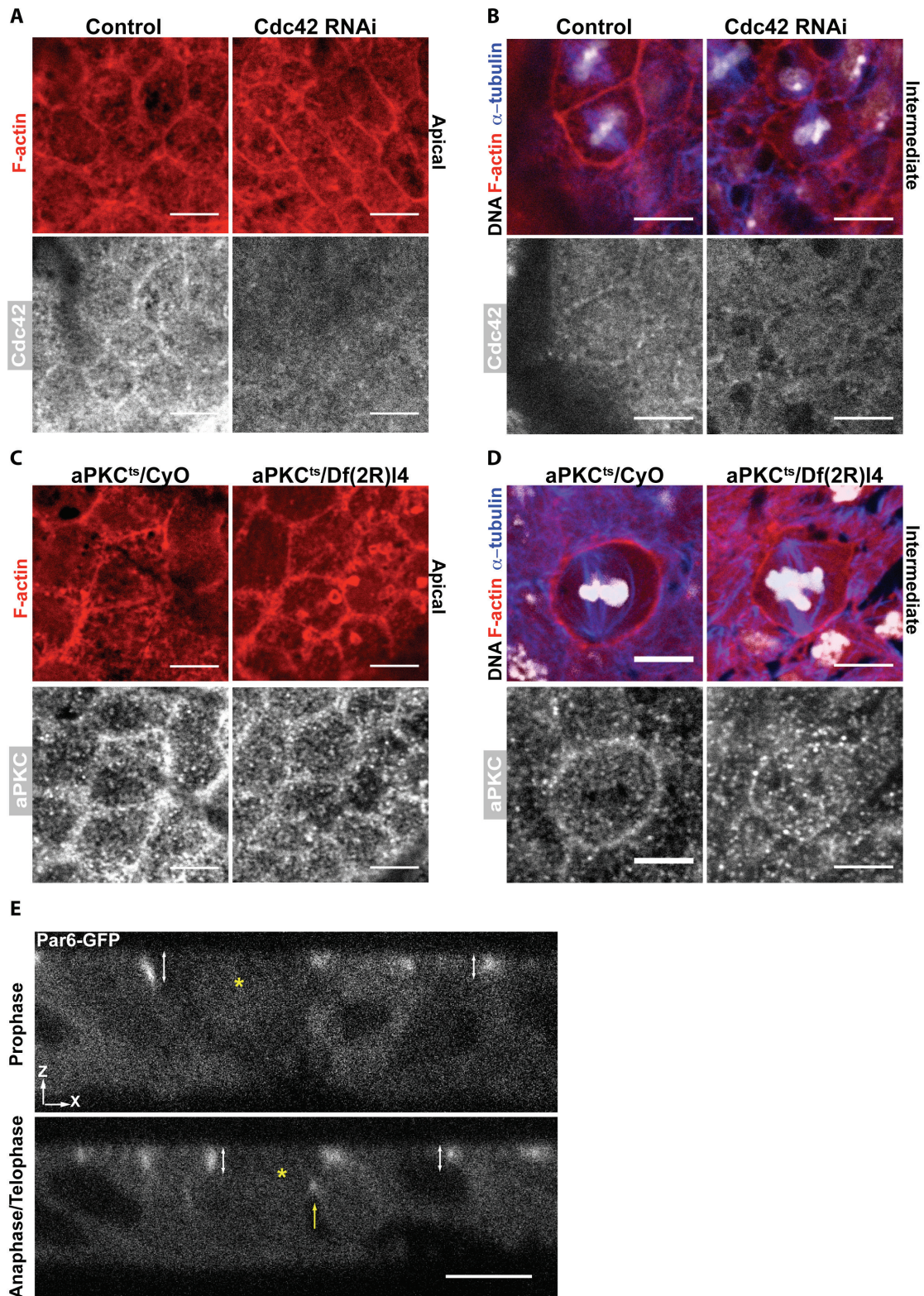


**Figure S4. Lateral spreading of Cdc42, aPKC and Par6 during mitosis; Related to Fig.5. (A)** Cdc42 RNAi cells labelled for F-actin (red) and using anti-Cdc42 antibody (white) imaged in xy at an apical plane of the epithelium. **(B)** A mitotic Cdc42 RNAi cell stained for F-actin (red), DNA (white),  $\alpha$ -tubulin (blue) and Cdc42 (white). **(C)** Control (*aPKC<sup>ts</sup>/CyO*) and homozygous *aPKC<sup>ts</sup>*



mutant tissue (*aPKC<sup>ts</sup>/Df(2R)14*) labelled for F-actin (red) and aPKC (white) and imaged in xy at the apical plane of the tissue. **(D)** As in C but stained for F-actin (red), DNA (white),  $\alpha$ -tubulin (blue) and aPKC (white) to show mitotic cells in xy at the spindle plane. **(E)** Live imaging of a cell expressing Par6-GFP at prophase and anaphase/telophase in cross-section (xz). White double arrow marks polarized interphase Par6::GFP. Yellow asterisk marks dividing cell. Yellow arrow marks cleavage furrow. Scale bar: 5 $\mu$ m.

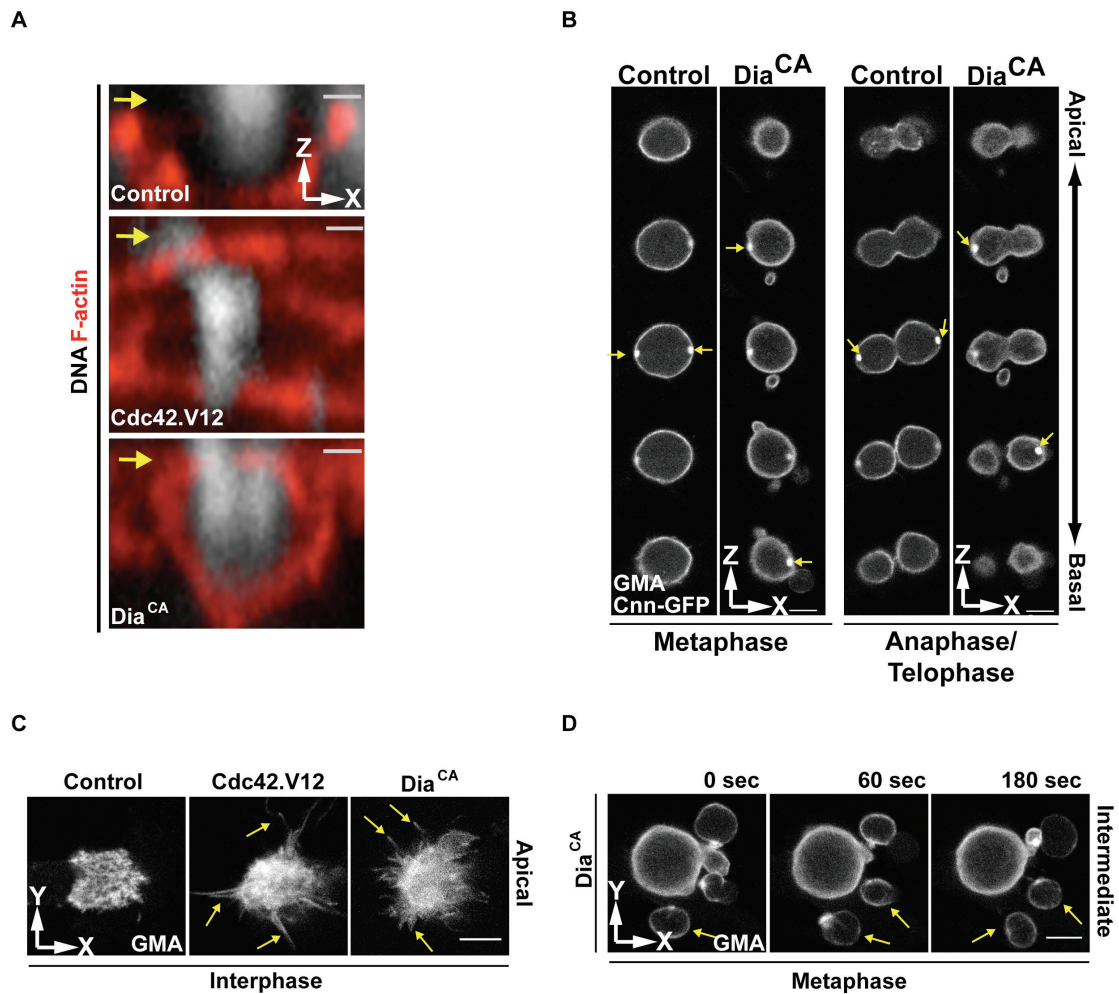


**Figure S5. Constitutively active forms of Cdc42 and Dia are sufficient to drive apical filament formation in mitosis; Related to Fig.6. (A)** Cross section of control, Cdc42.V12 and Dia<sup>CA</sup> expressing cells in metaphase labelled for F-actin (red) and DNA (white). Note apical actin-rich cortex in Cdc42.V12 and Dia<sup>CA</sup> cells (yellow arrow). Scale bar: 1.3  $\mu$ m. **(B)** Confocal sections of plane of the tissue (xy) taken from apical to basal for control and Dia<sup>CA</sup> expressing SOP cells marked with UAS-GMA::GFP and UAS-CNN::GFP in metaphase and telophase. Yellow arrows mark centrosomes. Scale bar: 5  $\mu$ m. **(C)** Apical section in plane of epithelium (xy) of actin in control, Cdc42.V12 and Dia<sup>CA</sup> expressing SOP cells in interphase marked with UAS-GMA::GFP. Yellow arrows mark actin-rich protrusions. Scale bar: 5  $\mu$ m. **(D)** Time-lapse movie of a mitotic Dia<sup>CA</sup> expressing SOP cell imaged in xy at the level of the spindle using UAS-GMA::GFP. Yellow arrows mark blebs that have been pinched off. Scale bar: 5  $\mu$ m.

## Supplemental Experimental Procedures

### Fly Stocks

RNAi lines used to silence the expression of the following genes: *cdc42* (NIG-Fly library, ID 12530R-3), *aPKC* (VDRC-Fly library, ID 105624), *arp3* (VDRC-Fly library, ID 35260), *diaphanous* (VDRC-Fly library, ID 103914), *pebble* (VDRC-Fly library, ID 109305), *par-6* (VDRC-Fly library, ID 19731).

### Dissections and live imaging

The expression of Neu-GMA was used to label actin filaments in P1 cells (Cohen et al., 2010); UAS-Tub::RFP was expressed from the *pnr* promoter to label microtubules in epithelial cells; UAS-Lifeact::GFP was expressed from the *pnr* promoter to label actin filaments in epithelial cells. The Neu-Gal4 driver was used to express UAS-CNN::GFP, UAS-GMA and UAS-Dia<sup>CA</sup> in P1 cells. RNAi-induced gene silencing was accomplished by using the *pnr*-Gal4 driver to express Gal4-responsive hairpin dsRNAs in transgenic flies (Mummery-Widmer et al., 2009). In case of RhoDN, Cdc42.V12 and Dia<sup>CA</sup> transgenes and where the RNAi transgenes were toxic, the Gal80ts system was used to limit expression, after which flies were shifted to 29°C at 6-9 hours AP (Zeidler et al., 2004).

*apkc<sup>ts</sup>* zygotic mutant pupae were obtained by crossing the *apkc<sup>ts</sup>/CyO*, pAct5C-GFP stock with the Df(2R)l4/CyO, pAct5C-GFP and pupae were selected by the absence of GFP, whereas GFP-positive larvae were used as controls.

The following antibodies and dyes were used at the indicated dilutions for our study: Guinea Pig anti-Par6 1:500 (gift from Frank Pichaud); Rabbit anti-



aPKC $\zeta$  (c-20) 1:100 (Santa Cruz Biotechnonology); Rabbit pMyosin Light Chain II (S19) 1:30 (Cell Signaling Technology); Mouse anti- $\alpha$ -tubulin (clone DM1A) 1:250 (Sigma); Rabbit anti-Cdc42 1:20 (Eurogentec); Chicken anti-GFP 1:500 (Abcam); rabbit anti-V5 1:100 (Abcam); Rabbit anti-Dia 1:400 (Gift from Steven A. Wasserman); TRITC-conjugated Phalloidin 1:500; DAPI 1:1000. Secondary antibodies from Molecular Probes were labeled with Alexa 488, 546 and 647 dyes.

### **Expression vectors, Cell culture and Immunoprecipitation**

The Par6 and Pbl cDNA constructs were generated through the Gateway system (Invitrogen) using full-length *Drosophila* Par-6 and Pbl cDNA as template. Fragments were inserted in frame into the pAct5C vector (DGRC, Indiana University) to create C-terminal Flag-tagged and N-terminal HA-tagged constructs respectively. For transfection, cells were seeded at  $2 \times 10^6$  cells / 600  $\mu$ l in a 12 well plate and allowed to adhere overnight.

48h after transfection (Effectene, Qiagen), whole cell lysates were washed once with PBS and homogenized in lysis buffer (50mM Tris pH7.5, 150mM NaCl, 1% Triton X-100, 1mM EDTA) containing protease (Roche) and phosphatase (Sigma) inhibitor cocktail. Following centrifugation, 500  $\mu$ g of supernatant was immunoprecipitated with 5  $\mu$ g of antibody (rabbit anti-HA [abcam], rat anti-HA [Roche] or mouse anti-flag [Sigma]) in 500  $\mu$ l lysis buffer overnight at 4°C on a rotator. Protein A/G magnetic beads (Pierce, Thermo Scientific) were added, and the mixture was incubated for an additional 1h at 4°C. Beads/extracts were washed three times with BSA/lysis buffer solution followed by three washes in lysis buffer. Bound proteins were eluted from the

beads in 2x Laemmli buffer by boiling for 10 min before separation by SDS-PAGE. For Western Blot analysis, gels were blotted to a polyvinylidene difluoride membrane. Blots were then incubated in 5% milk for 30 min in PBS-0.1% Tween-20, in primary antibody (rabbit anti-HA [abcam], mouse anti-flag [Sigma] or rabbit anti-aPKC [Sigma]) overnight at 4°C, and finally in secondary antibody for 1h.

### **In vitro binding assay**

Recombinant GST::Cdc42 was produced in BL21-A1 *E. coli* by using the pDEST-15 vector (Invitrogen). 4 h after induction with 0.2% L-arabinose, cells were pelleted and resuspended in GST lysis buffer [50 mM Tris-HCl pH 7.6, 50 mM NaCl, 5mM MgCl<sub>2</sub>, 10 mM dithiothreitol (DTT), protease inhibitor cocktail Complete (Roche)]. Cells were sonicated and debris was removed by centrifugation at 9000 RPM for 15 min. Glutathione-Sepharose beads were incubated with the supernatant on a rotator for 30 min at 4°C. Beads were washed 5 times with GST storage buffer [50 mM Tris-HCl pH 7.6, 50 mM NaCl, 5mM MgCl<sub>2</sub>, 1 mM dithiothreitol (DTT), protease inhibitor cocktail Complete (Roche)], and stored in the same buffer. Production and purification of GST::Cdc42 proteins were verified by Coomassie staining of SDS/PAGE gel. GST-pull-down assays were performed by using 300 µl of Myc::Pbl transfected (or salmon sperm transfected as negative control) S2 cell lysates along with 5-30 µl of glutathione-Sepharose beads with bound GST-Cdc42. After 1h incubation with rotation at 4°C, the supernatant was removed and the beads were washed five times with lysis buffer (see immunoprecipitation for recipe). After SDS/PAGE, Pbl and recombinant GST proteins were detected

by Western blotting using anti-Myc (Santa Cruz) and anti-GST (Sigma) antibody.



## References

Cohen, M., Georgiou, M., Stevenson, N.L., Miodownik, M., and Baum, B. (2010). Dynamic filopodia transmit intermittent Delta-Notch signaling to drive pattern refinement during lateral inhibition. *Developmental cell* 19, 78-89.

Mummery-Widmer, J.L., Yamazaki, M., Stoeger, T., Novatchkova, M., Bhalerao, S., Chen, D., Dietzl, G., Dickson, B.J., and Knoblich, J.A. (2009). Genome-wide analysis of Notch signalling in *Drosophila* by transgenic RNAi. *Nature* 458, 987-992.

Zeidler, M.P., Tan, C., Bellaiche, Y., Cherry, S., Hader, S., Gayko, U., and Perrimon, N. (2004). Temperature-sensitive control of protein activity by conditionally splicing inteins. *Nature biotechnology* 22, 871-876.